Optimization of 1.3μm InAs/GaAs Quantum Dot Lasers Epitaxially Grown on Silicon: Taking the Optical Loss of Metamorphic Epilayers into Account

Jun Wang[1]*, Yiming Bai[2], Huiyun Liu[3], Zhuo Cheng[1], Mingchu Tang[3], Siming Chen[3], Jiang Wu[3], Konstantinos Papatryfonos[3], Zizhou Liu[3], Yongqing Huang[1], and Xiaomin Ren[1]

[1]State Key Laboratory of Information Photonics and Optical Communications, Beijing University of Posts and Telecommunications, Beijing 100876, China.
[2]State Key Laboratory of Alternate Electrical Power System with Renewable Energy Sources, North China Electric Power University, Beijing 102206, China.
[3]Department of Electronic & Electrical Engineering, University College London, London WC1E 7JE，UK.

*Email: wangjun12@bupt.edu.cn

Abstract

Taking the optical loss caused by the metamorphic layers into account, we have proposed an optimization strategy for 1.3 μm InAs/GaAs quantum dot (QD) laser structures directly grown on silicon. We have investigated the effects of QD layer number, the thickness and composition of AlGaAs cladding layers on QD laser performance. The results demonstrate, from the view of the net modal gain and the differential quantum efficiency, the optimized QD layer number is 7 for lasers grown on silicon, which is different from the optimized number of 5 for the counterparts grown on native substrates. The optimized thickness is obtained for the cladding layers of $Al_{0.4}Ga_{0.6}As$, $Al_{0.6}Ga_{0.4}As$ and $Al_{0.8}Ga_{0.2}As$. Further, the optimized QD layer number for the net modal gain is nearly independent of the material gain of active regions. More importantly, the optimization strategy provides a comprehensive method to understand the differences in design between QD laser structures on silicon and those on native substrates.

Keywords: semiconductor lasers, quantum dot lasers, lasers on silicon.
PACS: 42.55.Px, 42.60.Da

1. Introduction

Driven by on-chip optical interconnects instead of electrical links, silicon (Si) photonics has attracted increasing attention due to its potential prospects in applications [1-3]. Although some of the Si-based optical devices have demonstrated their techno-economic viability, a practical Si-based laser source remains a challenge for more than two decades due to the indirect bandgap of Si [4, 5].

Much effort has been made to realize laser sources on Si platform, such as Si Raman lasers [6], Si hybrid lasers [7], GeSi lasers on Si [8], and GeSn lasers on Si [9]. Among these efforts, the integration of III–V lasers monolithically grown on Si is considered to be a promising solution to obtain efficient light

sources on the Si platform in the near future [10-13]. However, direct epitaxial growth (metamorphic growth) of III–V semiconductors on Si wafers faces several significant difficulties including large mismatches in lattice constant, thermal expansion coefficient, and polar/non-polar heterointerface. These issues induce the formation of different types of defects, such as threading dislocations, thermal cracks and antiphase boundaries. Further, these defects can dramatically reduce the quality of III–V materials on Si as well as the performance of devices fabricated from them [14, 15].

Quantum dot (QD) lasers have shown promise for producing high performance lasers on Si with long lifetime due to the higher defect-tolerance than quantum well lasers. Hence, III–V QD lasers directly grown on Si have attracted increasing attention in recent years [12, 14, 16–19]. Some research groups studying on In(Ga)As/GaAs QD lasers epitaxially grown on Si have demonstrated impressive results. In 2005, a laser structure directly grown on Si was realized with a 5-layer QD active region and 1.5 µm n- and p-$Al_{0.4}Ga_{0.6}As$ cladding layers. The threshold current density and slope efficiency of 1.5 kA/cm^2 and 0.37 W/A were achieved at room temperature [16]. For 1.3 µm QD lasers grown on Si, a threshold current density of 725 A/cm^2 was achieved at room temperature, which includes a 5-layer InAs QD active region and 1.5 µm n- and p- $Al_{0.4}Ga_{0.6}As$ cladding layers. Then, the threshold current density was reduced to 62.5 A/cm^2 [17]. In 2014, a QD laser grown on Ge/Si substrates with a threshold current density of 427 A/cm^2 (16 mA/937×4 µm^2) and external quantum efficiency of 37% was achieved at room temperature. The laser structure includes a 7-layer InAs QD active region and 1.4 µm n- and p-$Al_{0.4}Ga_{0.6}As$ cladding layers [18]. In 2016, a room-temperature micro-disk laser with 5-layer QDs grown on Si (001) was realized, and the lasing threshold is similar to the threshold of identical lasers grown on native GaAs substrates [19-21].

Although many great progresses have been made in these works, the major research activities have been focused on the laser material growth and fabrication process. Seldom investigations have been developed on the optimization of the epitaxial material structures theoretically. Importantly, compared InAs QD laser structure grown on Si (metamorphic growth) with that grown on GaAs substrates, one of the significant differences is the high dislocation density in the former, which is generally more than 1.0×10^6 cm^{-2} in experiments [22, 23]. The dislocations degrade the internal quantum efficiency of active regions. However, another important issue easily to be ignored is the optical loss resulted from the dislocations through the mechanism of the electric micro-field at dislocation cores and optical scattering [24-26].

Especially for QD lasers directly grown on Si, the net modal gain and differential quantum efficiency are necessary to be improved through optimization of the epitaxial structures by taking the optical loss of dislocations into account. Obviously, a high net modal gain and differential quantum efficiency are the necessary requirements for the practical application of laser sources monolithically integrated on Si with a high density of components.

In this work, quantitatively considering the influence of the dislocation optical absorption, our purpose is to improve the net modal gain and differential quantum efficiency through optimizing the 1.3 µm InAs/GaAs QD laser structures grown on Si. The relationship between the net modal gain and the QD layer number is emphatically discussed. First, the dependence of the optical confinement factor on the QD layer number of the active region is investigated. Then, taking the dislocation optical loss into account, the material structure parameters for lasers on Si, including the Al-composition and thickness of AlGaAs cladding layers, have been analyzed in detail. Finally, to enhance the net modal gain and the differential quantum efficiency, the QD layer number is optimized quantitatively, and compared with the case of the laser structures grown on native substrates. The results demonstrate the optimal QD

layer number for laser structures on Si is 7, and is not similar to the layer number of 5 for that on native substrates.

2. Optical absorption of metamorphic layers on silicon

Compared with 1.3 µm InAs/GaAs QD laser structrues grown on native substrates, the counterparts with high dislocation density grown on Si not only have lower internal quantum efficiency, but also suffers a non-ignorable optical loss. For the former, the optical loss mainly derives from the free carrier absorption in both doped lower and upper cladding layers [27-30]. However, for the latter, in addition to the free carrier absorption, the optical absorption in metamorphic layers caused by high-density dislocations also contributes a significant part to the internal optical loss of the devices. Fig. 1(a) shows the optical absorption coefficient of the GaAs bulk and the GaAs/Si film in the wavelength range from 800 to 1600 nm measured by the previous experiments [24]. Comparing the two curves of the optical absorption coefficient in Fig. 1(a), we can find the optical absorption in GaAs/Si is much larger than that in GaAs bulk below the bandgap. The optical absorption below the bandgap is caused by the metamorphic layers of GaAs/Si, other than the Si substrate [24, 25]. The high-density dislocations and rough surfaces are the main reason of the optical absorption. According to the mechanism of electric micro-field, a theoretical method based on the dislocation density of metamorphic epilayers is proposed to estimate the optical absorption coefficient, and agreed well with the experimental results [24].

Because the optical absorption of AlGaAs materials by metamorphic growth has not been found in previous experiments, we calculated the optical absorption coefficient using the theoretical model proposed by Iber et al. [24]. Fig. 1(b) demonstrates the theoretical results and the experimental measurement of the GaAs/Si epilayer with a dislocation density of about 4.0×10^8 cm^{-2} obtained from Iber [24]. It is found the theoretical results are in line with the experiments well. The optical absorption coefficients of the three Al-composition AlGaAs/Si epilayers with a dislocation density of 1.0×10^6 cm^{-2} were calculated by the theoretical method, as shown in Fig. 1(b). The absorption coefficients of AlGaAs/Si epilayers are far lower than that of the GaAs/Si epilayers, because the dislocation density of the former (1.0×10^6 cm^{-2}) is much less than that of the latter. The theoretical results are in line with the experiments for the GaAs/Si epilayer. Hence, we believe the optical absorption coefficients of the AlGaAs/Si epilayers are also reliable.
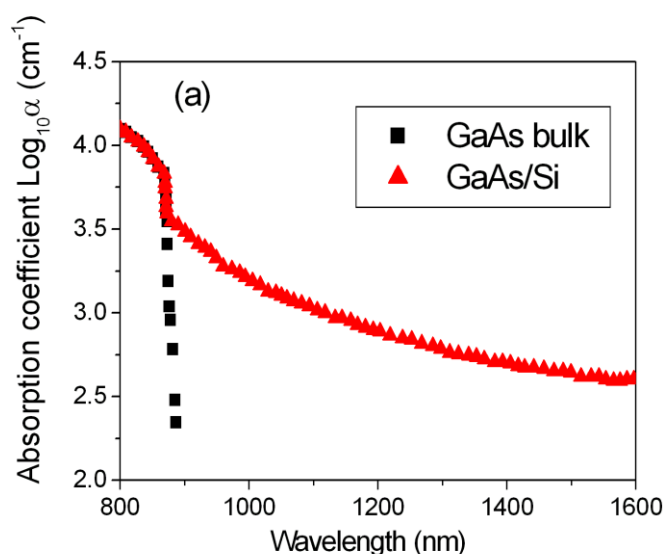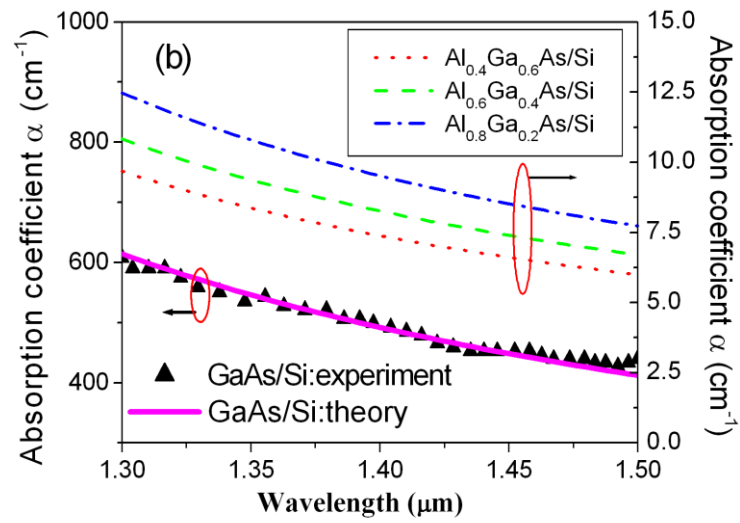
Fig. 1. (a) Optical absorption coefficient of the GaAs bulk and the GaAs/Si epilayer in experiments. (b) Theoretical results of the optical absorption coefficient of the three composition AlGaAs/Si epilayers with a dislocation density of 1.0×10^6 cm^{-2} and the GaAs/Si epilayer with the dislocation density of about 4.0×10^8 cm^{-2}. For comparison, the curve of experimental results for GaAs/Si epilayers is also plotted.

3. Laser structures on silicon and theoretical methods

In order to quantitively analyze the influence of metamorphic epilayer optical loss on lasers on Si, we take a common epitaxial structure as an example, as shown in Fig. 2. Fig. 2 presents the epitaxial structure of 1.3 µm InAs/GaAs QD lasers directly grown on Si. On a (001)-oriented Si wafer misoriented 4˚towards [110], it begins with a 1.0 µm GaAs buffer layer and a 1.0 µm dislocation filter layer. Then, it follows by a 0.5 µm n-doped GaAs contact layer. After that, an active region with multi-layer InAs/InGaAs/GaAs QDs is sandwiched by the doped lower and upper AlGaAs cladding layers. Each dot layer consists of 2.6 monolayers of InAs. Finally, it is ended with a 200 nm heavily doped GaAs layer as the p-side contact layer.

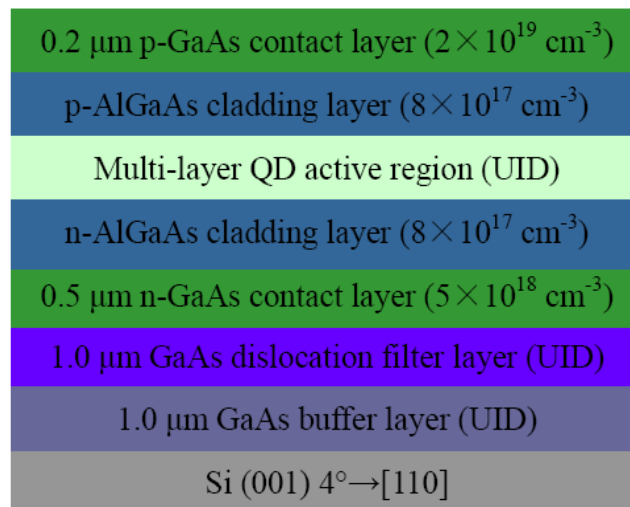Fig. 2. Schematic diagram of layer structure of 1.3µm InAs/GaAs QD lasers on Si.

The spacer layers separating the QD layers are considered to be 50 nm GaAs layers due to the requirement of strain accommodation for QDs, which is adopted by previous experiments [31-33]. The doping density in the AlGaAs cladding layers is assumed to be 8.0×10^{17} cm^{-3}, which dominates the optical internal loss in the laser structures on native substrates [30, 34]. To obtain a large net modal gain to realize low threshold current density and high external quantum efficiency, the QD layer number of the active region, the Al-composition and the thickness of the AlGaAs cladding layers are the three most important parameters to be optimized for the laser structures.

For the QD laser structures grown on Si, fewer QD layers and thinner AlGaAs cladding layers with lower Al-composition are preferable. In this theoretical investigation, to take the dislocation absorption and free carrier absorption into account, the extinction coefficient is considered as the imaginary part of the complex refractive index of the epilayers. The optical modal loss of the laser structures can be obtained from the imaginary part of the effective refractive index of the fundamental optical mode [28].

In a film waveguide structure, the Helmholtz equation with complex refractive index n can be written as

$$d^2 E(x) / dx^2 + k_0^2 [n^2(x) - n_{eff}^2] E(x) = 0,$$ (1)

where $k_0 = 2\pi/\lambda$ is the wave number, and n_{eff} is the effective refractive index. It is a one-dimensional differential equation yielding the eigenvalue n_{eff} and the electric field distribution E. The optical loss of the laser structure can be calculated form the imaginary part of the effective refractive index, using the relationship [28]

$$\alpha = 2 k_0 I_m (n_{eff}),$$ (2)

where $I_m(n_{eff})$ is the imaginary part of the effective refractive index. The optical confinement factor Γ is defined as the ratio of the integrated light intensity within the region of QDs to the total optical intensity throughout the laser structures

$$\Gamma = \int_{QD} |E|^2 dx / \int_{Total} |E|^2 dx .$$ (3)

The QD optical confinement calculation was performed by considering each QD layer as a quantum well with equivalent thickness of 2.6 monolayers of InAs.

In this work, the design of QD laser structures includes three main considerations: 1) The optical loss caused by the dislocation absorption and the free carrier absorption for lasers grown on Si [29, 30, 34]. 2) The dislocation absorption coefficient is obtained by the method mentioned above, as shown in Fig. 1(b), and the free carrier absorption coefficient is estimated by the common method [27, 34]. 3) The optical loss for the lasers caused by dislocation absorption and free carrier absorption is calculated by Eqs. (1) and (2) [28].

4. Results and discussion

To optimize the QD layer number, we firstly investigate the relationship between the optical confinement factor of QDs and the QD layer number for AlGaAs cladding layers with various Al-composition. The thickness of the AlGaAs cladding layers is chosen to be 2.0 μm to ensure enough optical confinement of the laser structures. The spacer layers which separate the QD layer are

considered to be 50 nm GaAs layers. The lower and upper waveguide layers are two 50-nm GaAs layers between QD layers and cladding layers. Hence, the thickness of the QD active region is decided by the QD layer number, e.g., the active region thickness is 50 × (N+1) nm for the N-layer QD laser structures. Fig. 3(a) shows the dependence of the optical confinement factor of all the QD layers on the QD layer number for different AlGaAs cladding layers. Further, Fig. 3(b) depicts the dependence of the average optical confinement factor per QD layer on the QD layer number ranging from 1 to 15. As seen from Fig. 3(a), the optical confinement factor increases rapidly with the QD layer number increasing when the QD layer number is less than 10 for different AlGaAs cladding layers. As the QD layer number is more than 10, the optical confinement factor increases slowly, and gradually to approach a same value for the three Al-composition AlGaAs cladding layers.

For the average optical confinement factor per QD layer, as shown in Fig. 3(b), it exhibits a peak for different AlGaAs cladding layers. The higher the Al-composition of AlGaAs cladding layers is, the higher the peak is. For the Al-composition of 0.4, 0.6 and 0.8, the QD layer number corresponding to the peak is 4, 4 and 3. If only from the view of optical confinement factor of the laser structures, the optimal QD layer number is 4, 4 and 3 for the three AlGaAs cladding layers.
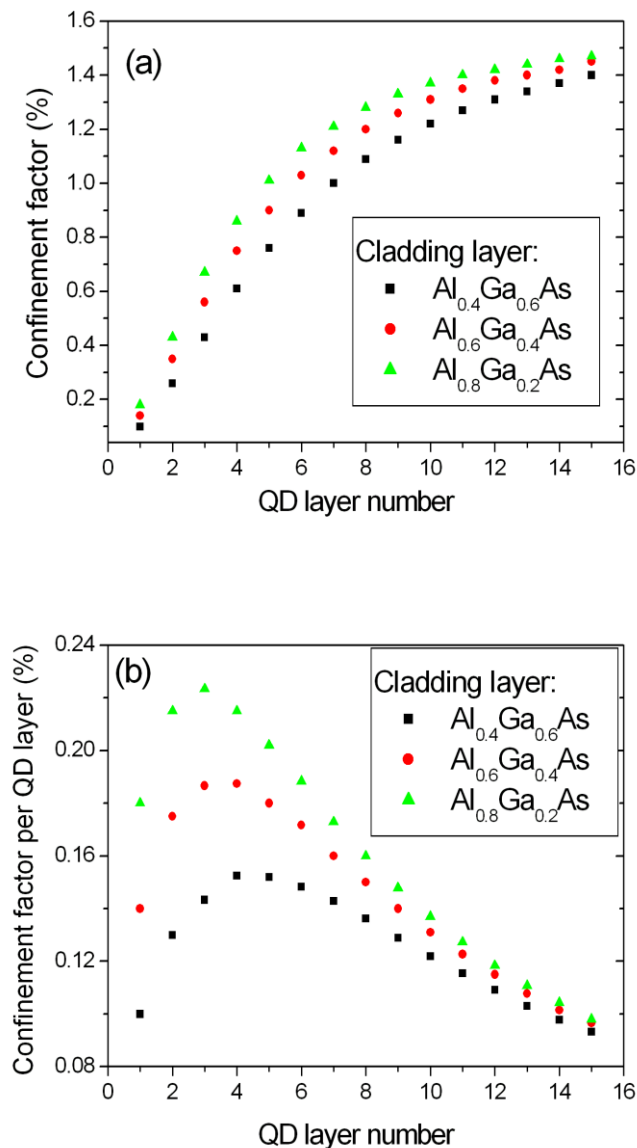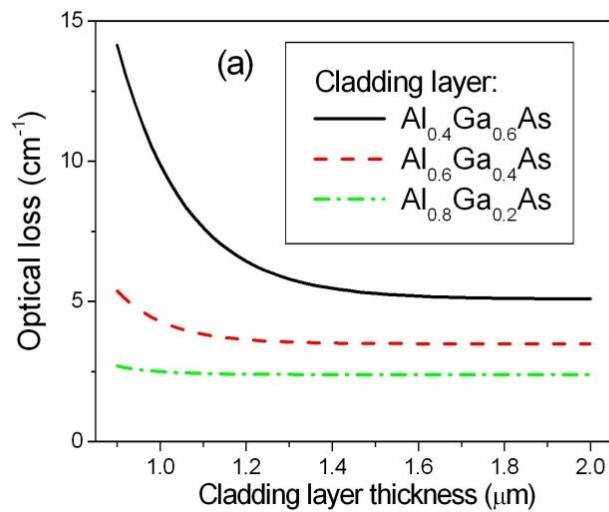
Fig. 3. Dependence of the optical confinement factor of total QD layers (a) and average optical confinement factor per layer (b) on the QD layer number with different AlGaAs cladding layers.

For the QD lasers on Si, we consider the internal optical loss mechanism derived from both dislocation absorption and free carrier absorption in the doped cladding layers and the outside layers, because the optical loss caused by QD layers and spacer layers is very small and can be neglected [28, 30]. To optimize the cladding layer thickness to decrease the optical modal loss, firstly, the active region thickness is fixed at 300 nm for the typical QD lasers grown on Si and native substrates. For simplicity, the dislocation density and the doping concentration in both the lower and the upper cladding layers of the laser structures on Si are considered to be 1.0×10^6 cm^{-2} and 8.0×10^{17} cm^{-3}. Fig. 4(a) depicts the dependence of the internal optical loss α_{in} on the cladding layer thickness for different Al-composition cladding layers. For the three cladding layers, the internal optical loss is decreased when the cladding layer becomes thicker. For the thinner cladding layers, the optical mode can further overlaps with the heavily doped layers in the outside of the cladding layers, and it causes higher optical loss.

From the three curves in Fig. 4(a), the internal optical loss is larger when the Al-composition of cladding layer is lower. It is noteworthy that the internal optical loss tends to be stability when the cladding layer thickness increases to 2.0 μm. Obviously, 2.0-μm cladding layer is too thick for optimal laser structures. Especially for the laser structures on Si, the cladding layers should be as thin as possible. When take the optical loss of the infinity cladding thickness as a reference, we define the optimal cladding thickness to meet the condition: $\alpha_{in}(\mathrm{d}_{opt}) / \alpha_{in}(\infty) - 1 \leq e^{-2}$. According to this definition, the optimized thickness is 1.5, 1.3 and 0.9 μm for the cladding layers of Al$_{0.4}$Ga$_{0.6}$As, Al$_{0.6}$Ga$_{0.4}$As and Al$_{0.8}$Ga$_{0.2}$As. Moreover, for the active region including the QD layer number ranging from 1 to 15, namely the active region thickness changes with the QD layer number, the optimal thickness of cladding layers with different Al-compositions is shown in Fig. 4(b). Hence, in the next analysis the thickness of the cladding layers is set as these optimized values.
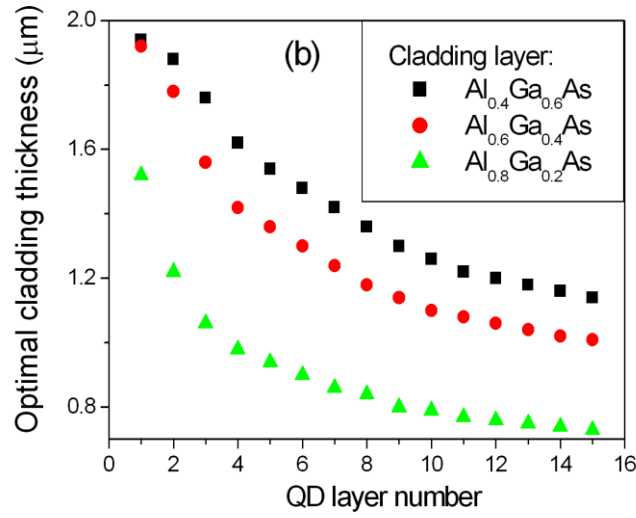
Fig. 4. (a) Optical loss versus the thickness of cladding layers with different Al-composition. (b) Dependence of the optimal thickness of cladding layers on the QD layer number with different Al-composition cladding layers.

The threshold current density is mainly decided by the net modal gain $G_m - \alpha_{in}$, for a constant device cavity length. According to the experimental results [35, 36], the material gain g_m is considered in the range from 2000 to 3000 cm^{-1} for InAs QD lasers. The modal gain G_m is the production of g_m and the optical confinement factor of QDs. In order to optimize the net modal gain of the lasers with the three Al-composition cladding layers, the material gain g_m is set to be 2500 cm^{-1} in the investigation firstly.

Fig. 5(a) depicts curves of the dependences of the average net modal gain per QD layer on the QD layer number for the laser structures on Si. There is a peak in each curve for the QD layer number ranging from 1 to 15. For the cladding layers with the Al-composition of 0.4, 0.6 and 0.8, the QD layer number corresponding to each maximum is 7, 7 and 6. The peak becomes higher for the case of the higher Al-composition cladding layers. Hence, for fewer QD layers, such as 7-QD layers, the Al-composition of the cladding layers has an obvious influence on the net modal gain. As the QD layer number is more than 10, the average net modal gain per layer tends to approach a same value for the three AlGaAs cladding layers.

Compared with the laser structures on Si, Fig. 5(b) shows the case of the counterparts on native substrates, also assuming the material gain g_m of 2500 cm^{-1}. There is also a peak in each curve. However, the QD layer number corresponding to each maximum is 5 for all the three AlGaAs cladding layers. When the QD layer number is more than 7, the average net modal gain per layer tends to approach a same value for the three cladding layers. Hence, the optimized QD layer number for the laser structures on Si and GaAs is different, and the optimal QD layer number for the former is more than that for the latter.

Further, for the both cases on Si and native substrates, it is important to be noted that the

optimized QD layer number for the net modal gain is not entirely in accord with that for the optical confinement factor of QDs. The reason comes from the optical loss which is also changeable with different QD active regions. Hence, from the view of average net modal gain, the 7-layer QDs is optimal for the lasers on Si with three AlGaAs cladding layers. For the QD laser structures on Si, fewer QD layers, lower Al-composition and thinner cladding layers are preferable. Also, considering the negative effects of higher growth temperatures needed for higher Al-composition epilayers, the optimized Al-composition for AlGaAs cladding layers should be compromised between the two mutually contradictory factors. Generally, the Al-composition of about 0.4 was commonly chosen in many experiments [12, 16-19, 23]. While, the $Al_{0.8}Ga_{0.2}As$ cladding layer was also used by adopting special growth skills in a few of reports [32].
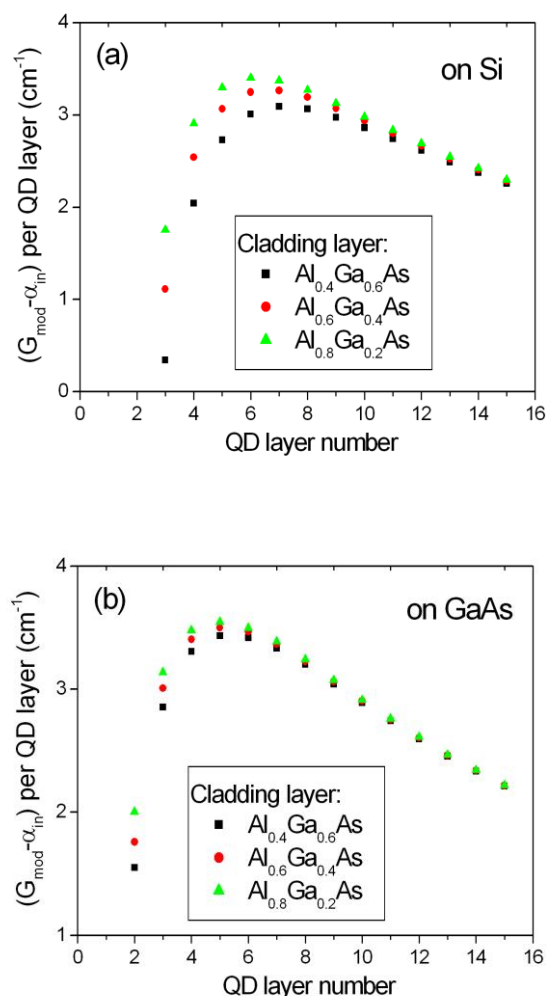

Fig. 5. Dependence of the net modal gain per layer on the QD layer number for the laser structures with different AlGaAs cladding layers on (a) Si and (b) native substrates.

Because the crystalline quality of QDs on Si is not good as that on native substrates, the material gain of the same laser structure grown on Si and native substrates is different. Hence, it is necessary to find the influence of the material gain on the average net modal gain per QD layer. Taking the laser structure with 1.5 μm $Al_{0.4}Ga_{0.6}As$ cladding layer as an example, here, three material gain levels of 2000, 2500 and 3000 cm^{-1} are considered, which cover the experimental results. Fig. 6 exhibits curves of the

dependences of the average net modal gain per layer on the QD layer number. There is a peak in each curve for the QD layer number ranging from 1 to 15 for the three material gain levels. The peak becomes higher for the case of the higher material gain level, and the QD layer numbers corresponding to the three peaks are the same value of 7. It indicates that the maximum of the average net modal gain per layer is nearly independent of the material gain ranging from 2000 to 3000 cm^{-1}, which represents the practical gain level in experiments. Furthermore, the behavior of the average net modal gain per layer is also similar to the cases of Al$_{0.6}$Ga$_{0.4}$As cladding layer and the Al$_{0.8}$Ga$_{0.2}$As cladding layer.
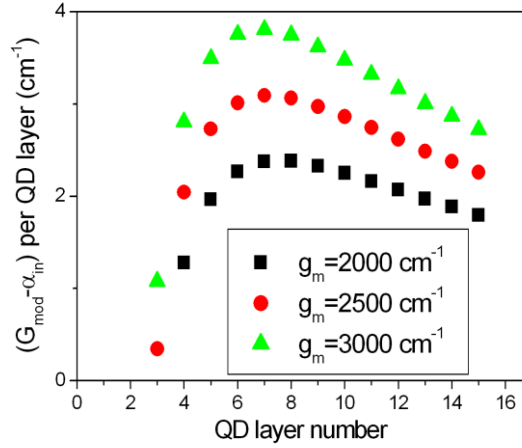

Fig. 6. Dependence of the net modal gain per layer on the QD layer number with different material gain levels.

The differential quantum efficiency is another important performance parameter of laser diodes, which indicates the percentage of electrons injected above the threshold that contributes photons to the laser beam. The efficiency is limited by the internal quantum efficiency, the net modal gain and the internal optical loss. Due to the high dislocation density of the laser materials grown on Si, the internal quantum efficiency η_i is lower than that of counterparts grown on native substrates. Generally, the former is only a half of the latter which is usually about 90% [10, 36]. Hence, for the lasers directly grown on Si, it is more important to improve the differential quantum efficiency for practical applications. The differential quantum efficiency η_d is decided by the relationship $\eta_d = \eta_i (G_m - \alpha_{in}) / G_m$. Because the internal quantum efficiency of the laser structures with different QD layers changes a little for the ground state emission in experiments (this hypothesis is just concluded approximatively from the experimental results, but not strictly correct in theory) [33, 37], here, the internal quantum efficiency η_i is considered to be a constant of 45% for the laser structure with different QD layer numbers. Fig. 7 shows the curves of the dependence of differential quantum efficiency on the QD layer number. The differential quantum efficiency increases rapidly with the QD layer number increasing when the QD layer number is less than 7 for different AlGaAs cladding layers. While, as the QD layer number is more than 7, the differential quantum efficiency tends to saturate for the three AlGaAs cladding layers. Hence, from the view of the differential quantum efficiency, the optimal QD number is 7 for the three AlGaAs cladding layers. To fairly compare experimental results with the calculated differential quantum

efficiency, the QD lasers on silicon with the similar epitaxial structure (typically shown in Fig. 2) and same growth technology (molecular beam epitaxy) should be considered properly. According to the reported experimental studies, three typical experimental results are suitable to extract for the comparison, as shown in Fig. 7 [18, 38, 39]. Seen from Fig. 7, the trend of the experimental results is in accord with the behavior of the calculation.
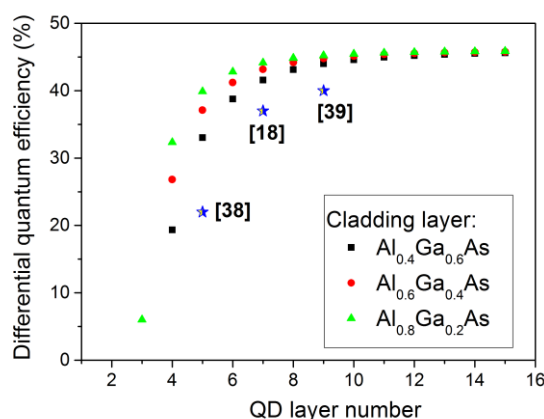

Fig. 7. Differential quantum efficiency versus the QD layer number with different AlGaAs cladding layers.

5. Conclusion

In summary, we have first proposed a structure optimization for 1.3 µm InAs/GaAs QD lasers directly grown on Si, taking the optical loss of dislocations into account. The QD layer number, thickness and composition of AlGaAs cladding layers are optimized in detail. The results demonstrate, for both laser structures on Si and native substrates, the optimized QD layer number for the net modal gain is not entirely in accord with that for the optical confinement factor of QDs. From the view of the net modal gain and the differential quantum efficiency, the optimized QD layer number is 7 for laser structures on Si, which is different from the optimized number of 5 for the counterparts on native substrates. Moreover, the optimized QD layer number for the net modal gain is nearly independent of the material gain. More importantly, the optimization design strategy provides a comprehensive way to understand the QD laser structures directly grown on Si. Furthermore, with the progress of the epitaxial growth technology on Si, we can achieve Si-based QD lasers with high performance, which will significantly promote the development of laser sources in silicon photonics.

References

[1] Rickman A 2014 The commercialization of silicon photonics *Nat. Photon*. **8** 579-582.

[2] Asghari M and Krishnamoorthy A 2011 Silicon photonics: energy-efficient communication *Nat. Photon.* **5** 268-270.

[3] Wang Z et al. 2015 Room-temperature InP distributed feedback laser array directly grown on silicon *Nat. Photon*. **9** 837-842.

[4] Liang D and Bowers J E 2010 Recent progress in lasers on silicon *Nat. Photon.* **4** 511-517.

[5] Chen R et al. 2011 Nanolasers grown on silicon *Nat. Photon*. **5** 170-175.

[6] Cloutier S G, Kossyrev P A and Xu J 2005 Optical gain & stimulated emission in periodic nanopatterned crystalline silicon *Nat. Mater.* **4** 887.

[7] Fang A W et al. 2006 Electrically pumped hybrid AlGaInAs-silicon evanescent laser *Opt. Express* **14** 9203-9210.

[8] Camacho-Aguilera R E et al. 2012 An electrically pumped germanium laser *Opt. Express* **20** 11316-11320.

[9] Stange D et al 2016 Optically Pumped GeSn microdisk lasers on Si *ACS Photon*. **3** 1279-1285.

[10] Zhou Z, Yin B and Michel J 2015 On-chip light sources for silicon photonics *Light Sci. Appl.* **4** 1-13.

[11] Tournié E et al. 2016 Metamorphic III-V semiconductor lasers grown on silicon *MRS Bulletin* **41** 218-223.

[12] Chen S et al. 2016 Electrically pumped continuous-wave III–V quantum dot lasers on silicon *Nat. Photon.* **10** 307-311.

[13] Wan Y et al. 2017 1.3 µm submilliamp threshold quantum dot micro-lasers on Si *Optica* **4** 940–944.

[14] Liu A Y et al. 2015 Reliability of InAs/GaAs quantum dot lasers epitaxially grown on silicon *IEEE J. Sel. Topics Quantum Electron.* **21** 690-697.

[15] Wang J et al. 2015 Extremely low-threshold current density InGaAs/AlGaAs quantum-well lasers on silicon *J. Lightwave Technol.* **33** 3163-3169.

[16] Mi Z, Bhattacharya R, Yang J and Pipe K P 2005 Room-temperature self-organised $In_{0.5}Ga_{0.5}As$ quantum dot laser on silicon *Electron. Lett*. **41** 742-744.

[17] Wang T, Liu H, Lee A, Pozzi F and Seeds A 2011 1.3 µm InAs/GaAs quantum-dot lasers monolithically grown on Si substrates *Opt. Express* **19** 11381-11386.

[18] Liu A Y et al. 2014 High performance continuous wave 1.3 µm quantum dot lasers on silicon *Appl. Phys. Lett.* **104** 041104.

[19] Wan Y et al. 2016 Optically pumped 1.3 µm room-temperature InAs quantum-dot micro-disk lasers directly grown on (001) silicon *Opt. Lett*. **41** 1664-1667.

[20] Wan Y et al. 2017 1.3 µm submilliamp threshold quantum dot micro-lasers on Si *Optica* **4** 940-944.

[21] Wan Y et al. 2017 O-band electrically injected quantum dot micro-ring lasers on on-axis (001) GaP/Si and V-groove Si *Opt. Express* **25** 26853-26860.

[22] Li Q et al. 2016 1.3 µm InAs quantum-dot micro-disk lasers on V-groove patterned and unpatterned (001) silicon *Opt. Lett*. **24** 21038 -21045.

[23] Liu A Y et al. 2017 Electrically pumped continuous-wave 1.3 µm quantum-dot lasers epitaxially grown on on-axis (001) GaP/Si *Opt. Lett.* **42** 338-341.

[24] Iber H, Peiner E and Schlachetzki A 1996 The effect of dislocations on the optical absorption of heteroepitaxial InP and GaAs on Si *J. Appl. Phys*. **79** 9273-9277.

[25] Peiner E, Mo S, Iber H, Tang G P and Schlachetzki A 1996 Characterization of thin buffer layers for strongly mismatched heteroepitaxy *Thin Solid Films* **283** 226-229.

[26] Zwinge G, Ziegenmeyer I, Wehmann H H, Tang G P and Schlachetzki A 1993 InP on Si substrates characterized by spectroscopic ellipsometry *J. Appl. Phys*. **74** 5889-5891.

[27] Bulashevich K A, Mymrin V F, Karpov S Y, Demidov D M and Ter-Martirosyan A L 2007 Effect of free-carrier absorption on performance of 808 nm AlGaAs-based high-power laser diodes Semicond. *Sci.*

Technol. **22** 502–510.

[28] Liu D C et al. 1993 Role of cladding layer thicknesses on strained-layer InGaAs/GaAs single and multiple quantum well lasers *J. Appl. Phys.* **73** 8027-8034.

[29] Haug A 1992 Free-carrier absorption in semiconductor lasers *Semicond. Sci. Technol.* 7 373-378.

[30] Smowton P M et al. 2001 Optical mode loss and gain of multiple-layer quantum-dot lasers *Appl. Phys. Lett.* **78** 2629-2631.

[31] Liu H et al. 2004 Improved performance of 1.3 μm multilayer InAs quantum-dot lasers using a high-growth-temperature GaAs spacer layer *Appl. Phys. Lett*. **85** 704-706.

[32] Maximov M V et al. 2008 A 1.33 μm InAs/GaAs quantum dot laser with a 46 cm^{-1} modal gain *Semicond. Sci. Technol*. **23** 105004.

[33] Kovsh A R et al. 2003 InAs/ InGaAs/GaAs quantum dot lasers of 1.3 μm range with enhanced optical gain *J. Cryst. Growth* **251** 729-736.

[34] Tan S et al. 2015 Graded doping low internal loss 1060-nm InGaAs/AlGaAs quantum well semiconductor lasers *Chin. Phys. B* **24** 064211.

[35] Liu A Y, Gossard A C, Bowers J E, Norman J and Srinivasan S 2015 Quantum dot lasers for silicon photonics *Photon. Res*. **3** B1-B9.

[36] Salhi A et al. 2007 High efficiency and high modal gain InAs/InGaAs/GaAs quantum dot lasers emitting at 1300 nm *Semicond. Sci. Technol.* **22** 396-398.

[37] Zhukov A E et al. 2003 High external differential efficiency and high optical gain of long-wavelength quantum dot diode laser *Physica E* **17** 589-592.

[38] Norman J et al. 2017 Electrically pumped continuous wavequantum dot lasers epitaxially grown on patterned on-axis (001) Si *Opt. Express* **25** 3927.

[39] Yang J, Bhattacharya P and Mi Z 2007 High-Performance In$_{0.5}$Ga$_{0.5}$As/GaAs Quantum-dot lasers on silicon with multiple-layer quantum-dot dislocation filters *IEEE T. Electron Dev*. **54** 2849-2855.